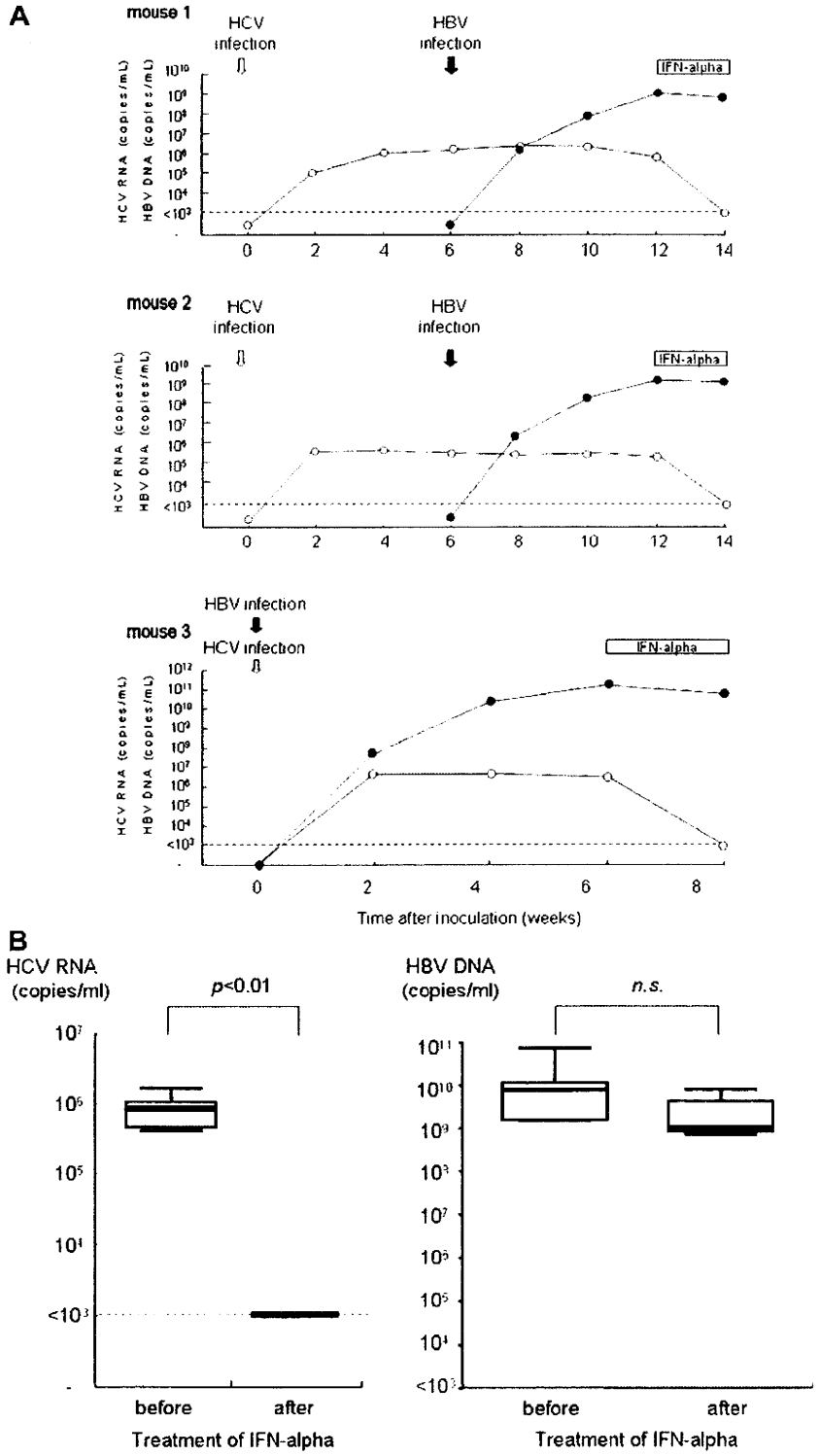

Fig. 3. Changes in serum hepatitis C virus (HCV) RNA and hepatitis B virus (HBV) DNA levels and effects of IFN on HBV–HCV-coinfected mice. Three mice (mouse 1, 2, and 3) were inoculated with both HBV- and HCV-positive human serum samples and treated daily with 7000 IU/g per day of interferon-alpha (IFN-α) intramuscularly for 2 weeks. Mice sera samples were obtained every 2 weeks after injection, and HCV RNA (open circles) and HBV DNA (close circles) were analyzed by quantitative polymerase chain reaction. (A) The horizontal dashed line represents the detectable limit (10^3 copies per milliliter). (B) Serum HCV RNA and HBV DNA titers in mice before and after 2-week IFN-α treatment. In these box-and-whisker plots, lines within the boxes represent median values; the upper and lower lines of the boxes represent the 25th and 75th percentiles, respectively.

Table 1
Hepatitis B virus (HBV) markers in supernatants of stable HBV-transfected cell lines.

Clone	HBsAg (IU/L)	HBeAg (IU/L)	HBV DNA (log copies per milliliter)
39	0.46	4.57	5.2
42	8.16	1.34	5.3
53	0.08	9.29	5.4

Abbreviations: HBsAg, hepatitis B surface antigen; HBeAg, hepatitis B e antigen.

evoking the IFN production system in liver cells. Further study using double-infected mice treated with anti-HBV nucleotide analogs and anti-HCV protease inhibitors should be conducted to confirm the present findings.

With regard to the use of IFN as a treatment, we initially assumed that HBV infection would prevent the effect of IFN on HCV and possibly vice versa in double-infection mice. Unexpectedly, the reduction of HCV by IFN therapy was quite similar in mice infected with HCV only and in those coinfected with HBV and HCV (Figs. 1 and 3). This finding indicated that HBV does not disturb the effect of IFN through signal transduction from the IFN receptor through the Jak-STAT pathway. It was, however, considered possible that HBV and HCV infect different liver cells in mice and replicated without being affected by each other. It has been reported that the same liver cell could be infected with both HBV and HCV [20,26], but it was difficult in the present study to confirm that these two viruses replicate in the same liver cell of mice because it is difficult to visualize HCV antigen and RNA in pathologic sections of the mouse liver. To address this issue, we transfected HCV to stable HBV-producing cell lines (Fig. 4). We thought that both HCV and HBV were produced from successfully HCV RNA transfected cells because transfected cells were stable HBV-producing cells. Presence of the both hepatitis viruses in the same hepatocytes has also been shown by a recent report by Bellecave et al. [20]. We showed in our cell line experiments that only HBV-transfected cell lines produced HBV and that cells cotransfected with HBV and HCV did not show a clear effect of HCV replication on HBV production (Fig. 4A). Similarly, stable production of HBV did not alter the replication of HCV (Fig. 4B). These data are consistent with a recent report [20] that showed that HCV could infect cells producing HBV and suggest a lack of interference between the two viruses in liver cells.

Using HCV-transfected HBV-producing cell lines, we demonstrated that presence of HBV did not disturb the actions of IFN on HCV (Fig. 5C). HCV utilizes certain machinery to disrupt the innate immune system; however, once exposed a large concentration of IFN, the virus shows high sensitivity, as shown in the replicon system [16,27]. Thus, HCV seems to have a relatively weak ability to disturb the antiviral actions of IFN compared with HBV. In contrast, HBV showed strong resistance against IFN in cells with diminished HCV replication [28]. The fact that HBV does not disturb IFN signaling but resists the actions of IFN suggests that HBV counteracts the actions of IFN at IFN-induced antiviral product levels.

Although the culture environment is different from the replicon system, the JFH1 strain seems relatively resistant to IFN [29]. This suggests that the core and envelope proteins, which are absent in the replicon system, might play a role in IFN resistance; however, we could not show any effect for HCV infection on the actions of IFN on HBV replication. This finding sug-

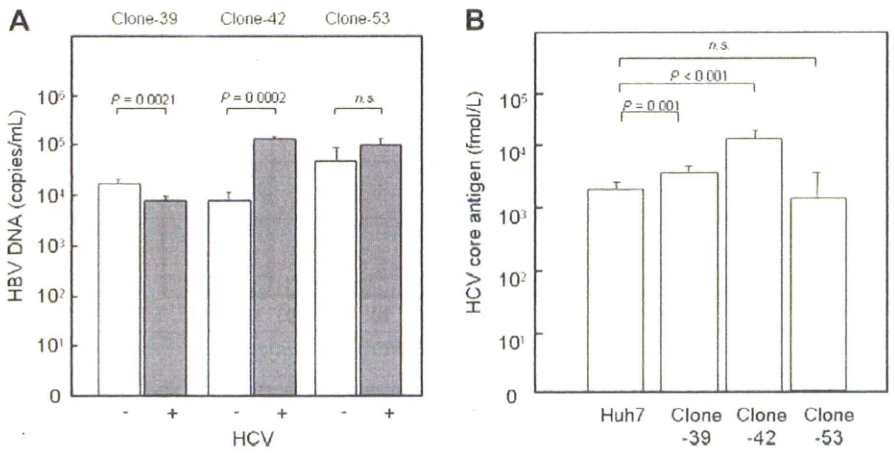

Fig. 4. Virus titers in supernatants of hepatitis B virus (HBV)–transfected or hepatitis C virus (HCV)–transfected cell lines. Huh7 cells were initially stably transfected with 1.4 genome-length HBV DNA. Three cell lines (Clone-39, -42, and -53) producing HBV DNA into the supernatant were selected. (A) HBV DNA levels in supernatants of HBV-producing cell lines 72 hours after transfection with JFH1 RNA (HCV positive) or control plasmid (HCV negative). (B) HCV core antigen levels in the supernatant of parental Huh7 cells and HBV-producing cell lines 72 h after transfection with JFH1 RNA. Data are mean plus or minus standard deviation ($n = 3$).

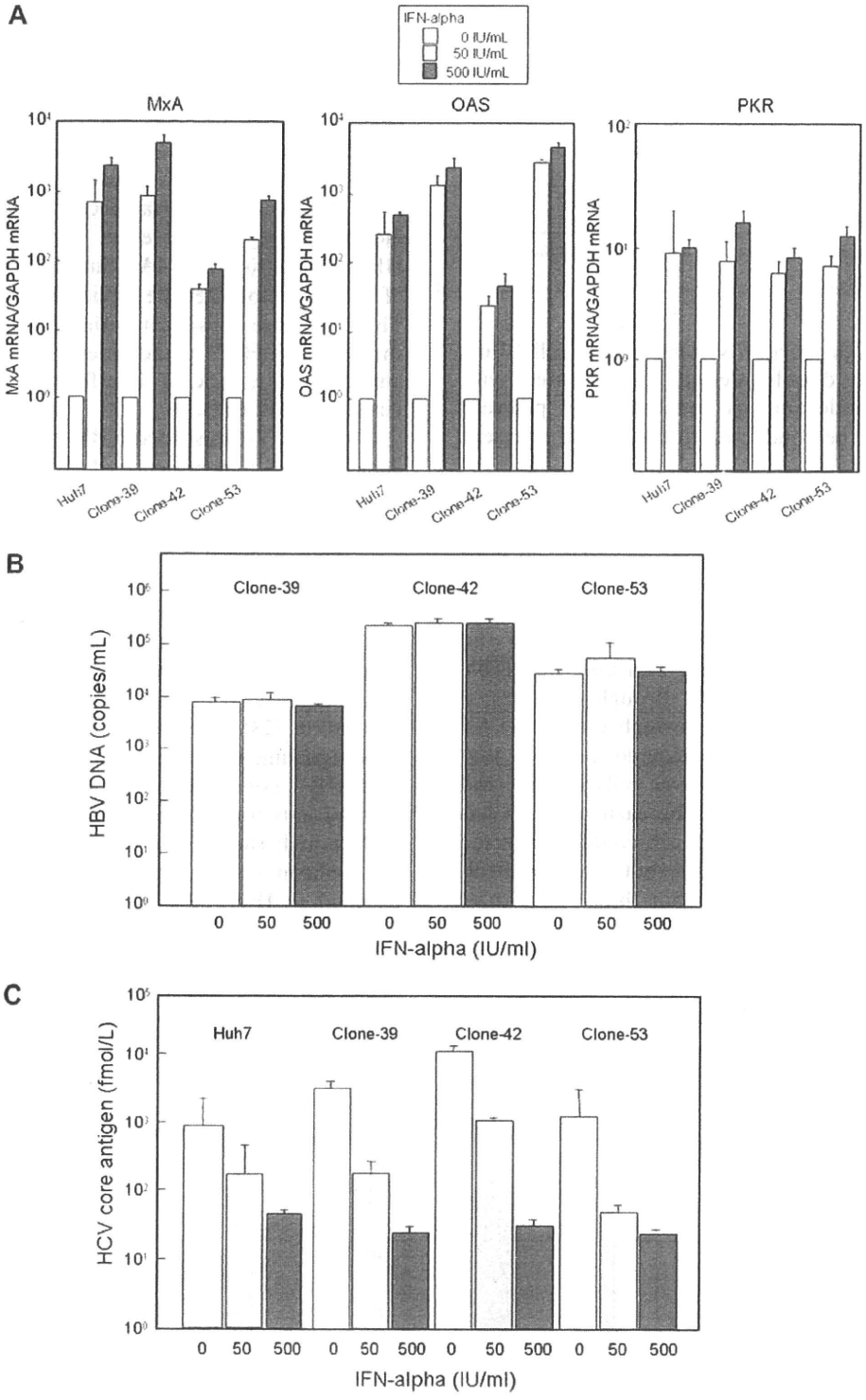

Fig. 5. Effects of interferon (IFN) treatment on hepatitis B virus (HBV) and hepatitis C virus (HCV) *in vitro*. Parental Huh7 cells and three HBV-transfected Huh7 cell lines (Clone-39, -42, and -53) were transfected with JFH1 RNA. Immediately after JFH1 transfection, the cell lines were treated with IFN-α (0, 50, and 500 IU/mL) for 72 h. (A) Intracellular gene expression levels of mixovirus resistance protein A (MxA), 2′,5′-oligoadenylate synthetase (OAS), and RNA-dependent protein kinase (PKR) were measured. RNA levels were expressed relative to glyceraldehydes-3-phosphate dehydrogenase (GAPDH) messenger RNA. (B) HBV DNA and (C) HCV core antigen in supernatants were measured. Data are mean plus or minus standard deviation ($n = 3$).

gests that the core and envelope proteins have only a weak effect on IFN resistance.

In clinical practice, HBV shows high resistance against IFN therapy. This is also the case in the cell culture system, as we showed in this study and has been reported in previous studies [20,28]. The mechanism by which hepatitis viruses resist IFN needs to be clarified in order to develop new and effective therapies for eradication of these viruses.

Acknowledgments

The authors thank Yoshie Yoshida, Kazuyo Hattori, and Rie Akiyama for their excellent technical help.

This study was supported in part by a Grant-in-Aid for Scientific Research from the Japanese Ministry of Labor and Health and Welfare.

References

[1] Maddrey WC. Hepatitis B: an important public health issue. J Med Virol 2000;61:362–366.
[2] Global surveillance and control of hepatitis C. Report of a WHO Consultation organized in collaboration with the Viral Hepatitis Prevention Board, Antwerp, Belgium. J Viral Hepat 1999;6:35–47.
[3] Beasley RP. Hepatitis B virus. The major etiology of hepatocellular carcinoma. Cancer 1988;61:1942–1956.
[4] Samuel CE. Antiviral actions of interferons. Clin Microbiol Rev 2001;14:778–809.
[5] Sagnelli E, Coppola N, Scolastico C, Filippini P, Santantonio T, Stroffolini T, et al. Virologic and clinical expressions of reciprocal inhibitory effect of hepatitis B, C, and delta viruses in patients with chronic hepatitis. Hepatology 2000;32:1106–1110.
[6] Chiaramonte M, Stroffolini T, Vian A, Stazi MA, Floreani A, Lorenzoni U, et al. Rate of incidence of hepatocellular carcinoma in patients with compensated viral cirrhosis. Cancer 1999;85:2132–2137.
[7] Cacciola I, Pollicino T, Squadrito G, Cerenzia G, Orlando ME, Raimondo G. Occult hepatitis B virus infection in patients with chronic hepatitis C liver disease. N Engl J Med 1999;341:22–26.
[8] Raimondo G, Brunetto MR, Pontisso P, Smedile A, Maina AM, Saitta C, et al. Longitudinal evaluation reveals a complex spectrum of virological profiles in hepatitis B virus/hepatitis C virus-coinfected patients. Hepatology 2006;43:100–107.
[9] Fried MW, Shiffman ML, Reddy KR, Smith C, Marinos G, Gonçales Jr FL, et al. Peginterferon alfa-2a plus ribavirin for chronic hepatitis C virus infection. N Engl J Med 2002;347:975–982.
[10] Liu CJ, Lai MY, Chao YC, Liao LY, Yang SS, Hsiao TJ, et al. Interferon alpha-2b with and without ribavirin in the treatment of hepatitis B e antigen-positive chronic hepatitis B: a randomized study. Hepatology 2006;43:742–749.
[11] Gotoh B, Komatsu T, Takeuchi K, Yokoo J. Paramyxovirus strategies for evading the interferon response. Rev Med Virol 2002;12:337–357.
[12] Evans JD, Seeger C. Cardif: a protein central to innate immunity is inactivated by the HCV NS3 serine protease. Hepatology 2006;43:615–617.
[13] Blindenbacher A, Duong FH, Hunziker L, Stutvoet ST, Wang X, Terracciano L, et al. Expression of hepatitis C virus proteins inhibits interferon alpha signaling in the liver of transgenic mice. Gastroenterology 2003;124:1465–1475.
[14] Bode JG, Ludwig S, Ehrhardt C, Albrecht U, Erhardt A, Schaper F, et al. IFN-alpha antagonistic activity of HCV core protein involves induction of suppressor of cytokine signaling-3. FASEB J 2003;17:488–490.
[15] Taylor DR, Shi ST, Romano PR, Barber GN, Lai MM. Inhibition of the interferon-inducible protein kinase PKR by HCV E2 protein. Science 1999;285:107–110.
[16] Frese M, Pietschmann T, Moradpour D, Haller O, Bartenschlager R. Interferon-alpha inhibits hepatitis C virus subgenomic RNA replication by an MxA-independent pathway. J Gen Virol 2001;82:723–733.
[17] Christen V, Duong F, Bernsmeier C, Sun D, Nassal M, Heim MH. Inhibition of alpha interferon signaling by hepatitis B virus. J Virol 2007;81:159–165.
[18] Su AI, Pezacki JP, Wodicka L, Brideau AD, Supekova L, Thimme R, et al. Genomic analysis of the host response to hepatitis C virus infection. Proc Natl Acad Sci USA 2002;99:15669–15674.
[19] Wieland S, Thimme R, Purcell RH, Chisari FV. Genomic analysis of the host response to hepatitis B virus infection. Proc Natl Acad Sci USA 2004;101:6669–6674.
[20] Bellecave P, Gouttenoire J, Gajer M, Brass V, Koutsoudakis G, Blum HE, et al. Hepatitis B and C virus coinfection: a novel model system reveals the absence of direct viral interference. Hepatology 2009;50:46–55.
[21] Tsuge M, Hiraga N, Takaishi H, Noguchi C, Oga H, Imamura M, et al. Infection of human hepatocyte chimeric mouse with genetically engineered hepatitis B virus. Hepatology 2005;42:1046–1054.
[22] Wakita T, Pietschmann T, Kato T, Date T, Miyamoto M, Zhao Z, et al. Production of infectious hepatitis C virus in tissue culture from a cloned viral genome. Nat Med 2005;11:791–796.
[23] Hiraga N, Imamura M, Tsuge M, Noguchi C, Takahashi S, Iwao E, et al. Infection of human hepatocyte chimeric mouse with genetically engineered hepatitis C virus and its susceptibility to interferon. FEBS Lett 2007;581:1983–1987.
[24] Tateno C, Yoshizane Y, Saito N, Kataoka M, Utoh R, Yamasaki C, et al. Near completely humanized liver in mice shows human-type metabolic responses to drugs. Am J Pathol 2004;165:901–912.
[25] Noguchi C, Ishino H, Tsuge M, Fujimoto Y, Imamura M, Takahashi S, et al. G to A hypermutation of hepatitis B virus. Hepatology 2005;41:626–633.
[26] Rodríguez-Iñigo E, Bartolomé J, Ortiz-Movilla N, Platero C, López-Alcorocho JM, Pardo M, et al. Hepatitis C virus (HCV) and hepatitis B virus (HBV) can coinfect the same hepatocyte in the liver of patients with chronic HCV and occult HBV infection. J Virol 2005;79:15578–15581.
[27] Blight KJ, Kolykhalov AA, Rice CM. Efficient initiation of HCV RNA replication in cell culture. Science 2000;290:1972–1974.
[28] Hayashi Y, Koike K. Interferon inhibits hepatitis B virus replication in a stable expression system of transfected viral DNA. J Virol 1989;63:2936–2940.
[29] Miyamoto M, Kato T, Date T, Mizokami M, Wakita T. Comparison between subgenomic replicons of hepatitis C virus genotypes 2a (JFH-1) and 1b (Con1 NK5.1). Intervirology 2006;49:37–43.

Cell Transplantation, Vol. 18, pp. 665–675, 2009
Printed in the USA.

0963-6897/09 $90.00 + .00
E-ISSN 1555-3892
www.cognizantcommunication.com

Hepatocytes From Fibrotic Liver Possess High Growth Potential in Vivo

Manabu Nishie,*† Chise Tateno,*[1] Rie Utoh,*[2] Toshihiko Kohashi,‡
Norio Masumoto,*‡ Naoya Kobayashi,† Toshiyuki Itamoto,‡ Noriaki Tanaka,†
Toshimasa Asahara,‡ and Katsutoshi Yoshizato*§[1]

*Yoshizato Project, CLUSTER, Hiroshima Prefectural Institute of Industrial Science and Technology, Hiroshima 739-0046, Japan
†Department of Surgery, Okayama University Graduate School of Medicine and Dentistry, Okayama 700-8558, Japan
‡Department of Surgery, Division of Frontier Medical Science, Program for Biomedical Research, and Hiroshima University 21st Century COE Program for Advanced Radiation Casualty Medicine, Graduate School of Biomedical Sciences, Hiroshima University, Hiroshima 734-8551, Japan
§Developmental Biology Laboratory and Hiroshima University 21st Century COE Program for Advanced Radiation Casualty Medicine, Department of Biological Science, Graduate School of Science, Hiroshima University, Hiroshima 739-8526, Japan

Hepatocyte transplantation is effective for treating liver failure, but healthy donors as a source of hepatocytes are quite limited. The livers of patients with hepatic fibrosis could be an alternative source; however, few reports have examined the nature of hepatocytes from fibrotic livers (f-hepatocytes). In this study, we compared the growth of f-hepatocytes and hepatocytes from normal livers (n-hepatocytes). Hepatocytes were isolated from normal and CCl_4-treated wild-type Fischer rats that express dipeptidyl dipeptidase IV (DPPIV) gene ($DPPIV^+$). The n- and f-hepatocytes proliferated in culture at similar rates. Both types of hepatocytes were transplanted into $DPPIV^-$ mutant Fischer rats that had been treated with retrorsine to injure the liver and were partially hepatectomized (PHx) before transplantation. Both n- and f-$DPPIV^+$-hepatocytes proliferated and formed colonies. The colony sizes of f-hepatocytes 21 days posttransplantation were approximately three times those of n-hepatocytes. The hepatocytes were analyzed using a fluorescence activated cell sorter (FACS). The FACS profile differed between f- and n-hepatocytes: f-hepatocytes were less granular, less autofluorescent, and smaller than n-hepatocytes. These characteristics of f-hepatocytes resembled those reported for small-sized n-hepatocytes (SHs), which are highly proliferative and preferentially express a unique set of 10 SH genes. However, f-hepatocytes preferentially expressed only five of the SH genes. The expression profile of f-hepatocytes was rather similar to that of proliferating n-hepatocytes in the regenerating liver after PHx. The f-hepatocytes were morphologically normal and did not show any preneoplastic phenotype. These normal and proliferative natures of f-hepatocytes in vivo suggest the fibrotic liver as a source of hepatocytes for transplantation.

Key words: Hepatocyte transplantation; Liver regeneration; Hepatocyte proliferation; Hepatectomy; Retrorsine; Carbon tetrachloride

INTRODUCTION

The liver cell transplantation therapy for a damaged liver was first reported in 1993, in which hepatocytes ($1–60 \times 10^7$ cells) were autotransplanted into the spleen of cirrhosis or chronic hepatitis patients (11). The donor cells lived for up to 11 months. Strom et al. transplanted less than 1.2×10^9 allogeneic hepatocytes into the spleen as a bridge to the ensuing liver transplantation (14). The patients who received hepatocyte transplantation before liver transplantation had an average survival of 3.8 ± 3.3 days versus 2.8 ± 2.5 days for those without hepatocyte transplantation. Although the survival period did not differ statistically, hepatocyte transplantation improved serum ammonia, cerebral blood flow, and intracranial pressure. Two of 30 patients were able to recover with hepatocyte transplantation alone without usual liver transplantation (14).

Patients with metabolic diseases have been also subjected to hepatocyte transplantation in some cases. For

Received October 31, 2008; final acceptance March 30, 2009.
[1]Present address: PhoenixBio Co., Ltd., PhoenixBio. Co. Ltd., 3-4-1 Kagamiyama, Higashishiroshima, Hiroshima 739-0046, Japan.
[2]Present address: Tokyo Women's Medical University, Institute of Advanced Biomedical Engineering and Science, Kawada-cho 8-1, Shinjuku-ku, Tokyo 162-8666, Japan.
Address correspondence to Katsutoshi Yoshizato, Ph.D., PhoenixBio. Co. Ltd., 3-4-1 Kagamiyama, Higashishiroshima, Hiroshima, 739-0046, Japan. Tel: 81-82-431-0016; Fax: 81-82-431-0017; E-mail: katsutoshi.yoshizato@phoenixbio.co.jp

example, an ornithine transcarbamoylase (OTC)-deficient 5-year-old patient was transplanted with 1.7×10^9 normal hepatocytes. The patient improved symptomatically but died from pneumonia 43 days posttransplantation (15). When a 10-year-old patient with Crigler-Najjar syndrome was transplanted with 7.5×10^9 hepatocytes, an amount approximately equal to 5% of the entire liver, the patient was able to decrease the serum bilirubin to a half the level before liver transplantation (4). Recently, a patient with glycogen storage disease type Ib caused by a deficiency of glucose-6-phosphate transporter was treated with hepatocyte transplantation, which resulted in normalization of glucose-6-phosphatase activity in the liver, and substantial improvement in quality of life (9).

These previous studies show that the transplantation of hepatocytes equivalent to 1–5% of the total hepatocytes in the liver is therapeutically effective. Cell transplantation is easier, safer, and less expensive than liver transplantation, and can be performed repeatedly. The major challenge to hepatocyte transplantation is the shortage of transplantable cells owing to the limited availability of healthy donors (16). Hepatocytes from fibrotic livers (f-hepatocytes) are a potential source of hepatocytes for transplantation because of their greater availability over hepatocytes from normal livers (n-hepatocytes). Mito et al. isolated n- and f-hepatocytes from rats and transplanted each of them into the syngenic rat spleen (10). Although the yield and viability of the f-hepatocytes were lower than the n-hepatocytes, and their features were different from the normal counterpart in some aspects, they were able to continue to proliferate for 6 months after transplantation. However, the proliferative ability of f-hepatocytes has not been characterized in the liver, which is of prime importance when they are utilized as the cells for transplantation.

This study aimed to characterize the growth of f-hepatocytes using rats as a model animal. The adult rat liver contains a minor population of hepatocytes called small hepatocytes (SHs) (6,17,19). These cells are smaller and have greater replicative potential than typical parenchymal hepatocytes (PHs). SHs have been characterized using an "SH fraction" that contaminated PHs. Previously, we isolated a PH-free SH fraction and SH-free PH fraction from the adult rat liver using a fluorescence-activated cell sorter (FACS) combined with centrifugal elutriation and characterized the hepatocytes in the fraction. These hepatocytes were designated as pure SHs or R3Hs and pure large hepatocytes (LH) or R2Hs in our previous study, respectively (2). For the sake of simplicity, we call pure SHs 'SHs" and pure LHs "LHs" in this study and assume that "hepatocytes" consist of LHs and SHs. SHs were mononuclear and of lower ploidy. Previously, we identified 10 genes that are preferentially expressed in SHs: *p55cdc, hydroxysteroid sulfotransferase (Sta), cytochrome P450 17 (CYP17), prostaglandin E2 receptor EP3 subtype (Pge2r), pancreatic secretory trypsin inhibitor (Psti), Cdc2, connexin 26 (Cx26), mitotic centromere-associated kinesin (Mcak), rat EST 207254*, and an unknown gene (*ab088476*) (2). These genes are referred to as the SH-associated genes.

We isolated n- and f-hepatocytes from rats. The f-hepatocytes were characterized in terms of size, FACS profile, in vitro and in vivo proliferation ability, and gene expression, and were compared with n-hepatocytes and hepatocytes in the regenerating liver (r-hepatocytes). As a result, we clearly demonstrated that f-hepatocytes are different from LHs, are similar to SHs in proliferation ability, and are similar to r-hepatocytes in their gene expression profile.

MATERIALS AND METHODS

Treatment of Animals

Dipeptidyl dipeptidase IV-deficient ($DPPIV^-$) mutant male Fischer rats aged 9–10 weeks were purchased from Charles River Japan, Inc. (Yokohama, Japan) and their wild-type ($DPPIV^+$) counterparts from Japan SLC, Inc. (Shizuoka, Japan). Liver fibrosis was induced by intramuscular injection of $DPPIV^+$ rats with CCl_4 at 1 ml/kg body weight, twice a week, for 6 weeks. Hepatocytes were isolated from the rats 6 weeks postinjection. $DPPIV^+$ male Fischer rats aged 15–16 weeks were subjected to two thirds partial hepatectomy (PHx). Then, r-hepatocytes were isolated from the rats 36 h after PHx.

Hepatocyte Isolation

$DPPIV^+$ male Fischer rats aged 15–16 weeks were divided into three groups, one used for normal controls, second for CCl_4 treatment, and the last for PHx experiment. The n-, f-, and r-hepatocytes were isolated from these rats using the two-step collagenase perfusion method (6), and were collected by centrifugation at $50 \times g$ for 2 min. The pellets were centrifuged through 45% Percoll at $50 \times g$ for 24 min (6). These pellets were centrifuged again at $50 \times g$ for 2 min, and the final pellets were used as hepatocytes, which consisted of LHs and SHs. In our previous study, PHs and SHs were obtained as the pellet and supernatant, respectively, after centrifugation of the original hepatocyte preparations at $50 \times g$ for 1 min (17). The hepatocyte preparation used in the present study corresponds to this previous preparation consisting of PHs and SHs. The viability of the hepatocytes was determined by Trypan blue exclusion. The n-, f-, and r-hepatocytes were subjected to FACS analysis, and to determining the cell diameter (17) and the gene expression levels. In addition, the proliferation ability of n- and f-hepatocytes was assayed in vitro and in vivo.

FACS Analysis

Hepatocytes were analyzed using a cell sorter (FACS Vantage; Becton Dickinson, Mountain View, CA) with a 100-μm nozzle, as reported previously (17). Fluorescence excited at 488 nm was measured through 530-nm (FL1) and 575-nm (FL2) filters with 4-decade logarithmic amplification. To measure the physical characteristics of the cells, linear amplification was used for the forward scatter, which is a measure of cell size, and 4-decade logarithmic amplification was used for the side scatter (SCC), which is a measure of cytoplasmic complexity. The optical bench was calibrated at a fixed amplitude and photomultiplier voltage using fluorescent polystyrene beads (Fluorosbrite Calibration Grade 6-μm YG microspheres; Polysciences, Warrington, PA), and the instrument was used in the conditions under which these beads fell in the same peak channels. Propidium iodide was added to the cell suspensions to be analyzed, at a concentration of 1 μg/ml. The cells that excluded the dye were analyzed as viable cells. Data obtained from the FACS experiments were analyzed using Cell Quest software (Becton Dickinson).

Determination of the Growth Potential of Hepatocytes In Vitro

The n- and f-hepatocytes were cocultured with mitomycin C-treated Swiss 3T3 cells on Celldesks in HCGM culture medium (i.e., Dulbecco's modified Eagle's medium supplemented with 10% fetal bovine serum, 20 mM *N*-2-hydroxyethylpiperazine-*N'*-2-ethane sulfonic acid, 30 μg/ml L-proline, 0.5 μg/ml insulin, 10^{-7} M dexamethasone, 44 mM $NaHCO_3$, 10 mM nicotinamide, 10 ng/ml EGF, 0.2 mM L-ascorbic acid 2-phosphate, 100 IU/ml penicillin G, and 100 μg/ml streptomycin) (1,13, 17–19). They were incubated in a 5% CO_2/95% air atmosphere at 37°C. Swiss 3T3 cells were seeded on the hepatocytes 24 h after the hepatocytes were plated. The growth potential of the hepatocytes was determined at 10 days, as previously shown (17).

Hepatocyte Transplantation

$DPPIV^-$ rats weighing 130–140 g were given two intraperitoneal injections of retrorsine at 30 mg/kg body weight, 2 weeks apart. Four weeks after the last injection, a two thirds PHx was performed (6,8). The n- and f-hepatocytes (1.5×10^5) isolated from the $DPPIV^-$ rats were transplanted into the retrorsine-treated partial hepatectomized (retrorsine/PHx) $DPPIV^-$ rats via the portal vein. Some rats were killed 48 h after transplantation to measure the engraftment rate of the transplanted hepatocytes, the ratio of transplanted cells to cells integrated to the liver plate. Other rats were killed 21 days after transplantation. Tissues from each lobe of the liver were frozen until use for enzyme-histochemical or immunohistochemical analyses.

Enzyme-Histochemical and Immunohistochemical Staining

DPPIV enzyme histochemistry was performed on 10-μm-thick cryosections that had been prepared from the liver, fixed in ice-cold acetone for 5 min, air-dried, and washed for 5 min in ice-cold 95% ethanol. The sections were air-dried and incubated for 40–60 min in a substrate reagent consisting of 0.5 mg/ml Gly-Pro-methoxy-β-naphthylamide (Sigma Chemical, St. Louis, MO), 1 mg/ml Fast Blue BB (Sigma Chemical), 100 mmol/L Tris-maleate (pH 6.5), and 100 mmol/L NaCl. Then, the sections were washed with PBS and fixed in 10% formaldehyde. All tissue sections were counterstained with hematoxylin.

Cryosections were fixed in −20°C acetone for 5 min and subjected to immunohistochemistry to detect liver-related proteins. The primary antibodies (Abs) used were as follows: anti-rat DPPIV mouse monoclonal antibody (gift from Dr. D. C. Hixson, Rhode Island Hospital), anti-rat albumin rabbit antiserum (a hepatocyte marker; Cappel, Durham, NC), anti-human α-smooth muscle actin (SMA) mouse monoclonal antibody (an activated stellate cell marker; MBL, Nagoya, Japan), anti-rat glutathione-*S*-transferase (a preneoplastic hepatocyte marker, GST-P) rabbit antiserum (MBL), OV6 mouse monoclonal antibody (an oval cell marker; gift from Dr. D.C. Hixson) (5), and anti-human cytokeratin 19 monoclonal antibody (CK19; a bile duct cell and oval cell marker; Amersham). The primary Abs were visualized with Alexa 488-labeled goat anti-mouse-IgG or Alexa 594-labeled goat anti-rabbit IgG (Molecular Probes, Eugene, OR).

Morphometric Analysis

Livers were isolated from rats 48 h after transplantation, weighed, and processed for cryosectioning and DPPIV staining. The approximate numbers of hepatocytes per gram of liver were calculated from the liver weight using the value $115 \times 10^6 \pm 15 \times 10^6$ hepatocytes/g liver (12). $DPPIV^+$ and $DPPIV^-$ hepatocytes were counted in arbitrary areas visualized on tissue sections, and the numerical ratio of the former to the latter was calculated as the occupancy rate of engrafted hepatocytes in the liver. The number of engrafted hepatocytes per liver was calculated by multiplying the occupancy rate of the engrafted hepatocytes by the total number of host hepatocytes per liver. The engraftment index (the numerical ratio of engrafted hepatocytes to injected hepatocytes on transplantation) was calculated by dividing the number of engrafted hepatocytes per liver by the number of injected hepatocytes.

A transplanted hepatocyte homes to the liver, starts to replicate there, and forms a colony soon after transplantation. The area of colonies formed by the transplanted hepatocytes was measured using NIH image var. 1.62, and the data were analyzed using StatView ver. 5.0 (SAS Institute, Cary, NC). The colony size increases as engrafted hepatocytes proliferate. The volume of a colony was estimated using a reported method (6). Briefly, we made 10-μm-thick semiserial sections from liver specimens, at 100-μm intervals. Different parts of a DPPIV$^+$ colony were seen in several different serial sections when the diameter of the colony exceeded 100 μm, which is a colony area corresponding to >7,850 μm^2. We selected the section in which the longest diameter of a particular DPPIV$^+$ colony was seen and calculated the colony area using this diameter. For a colony with a diameter <100 μm, we assumed that the diameter measured in a section was the longest diameter and calculated the colony area using this diameter. We only measured the colonies consisting of more than eight DPPIV$^+$ transplanted hepatocytes. The colonies were oval or round. To quantify the area of these colonies, 40 portal areas were examined in each animal at 21 days posttransplantation. The volume of a colony was calculated from the area of the colony, assuming that the colony was spherical and that the cross section was made along the maximum diameter of the sphere. To calculate the mean diameter of cells in colonies formed by the transplanted hepatocytes, the area and cell number therein were measured for 10 colonies. The mean cell number in a colony was calculated using the area or volume of the colony and the mean cell diameter of hepatocytes.

Quantification of mRNA

Total RNA was purified from n-, f-, and r-hepatocytes using an RNeasy minikit (QIAGEN K.K., Tokyo, Japan) and was treated with an RNase-free DNase set (QIAGEN). cDNA was synthesized using PowerScript reverse transcriptase (Clontech, Palo Alto, CA) and was amplified with a set of gene-specific primers (2) and SYBR Green PCR mix in a PRISM 7700 Sequence Detector (Applied Biosystems, Tokyo, Japan). A series of diluted plasmid cDNAs containing each gene was used to plot the standard amplification curves. The mRNA copy numbers in cDNA samples were calculated using the standard amplification curves (2).

Statistical Analysis

The area of colonies formed by the transplanted hepatocytes was measured using NIH image ver. 1.62, and the data were analyzed using StatView ver. 5.0 (SAS Institute, Cary, NC). The significance of differences was analyzed using the Mann-Whitney rank sum test. A value of $p < 0.05$ was considered significant.

RESULTS

Size and FACS Characterization of Hepatocytes

We prepared n- and f-hepatocytes from normal and CCl_4-treated rats, respectively. The yield of the n- and f-hepatocytes was $35.0 \pm 19.0 \times 10^6$ and $2.6 \pm 1.5 \times 10^6$ cells per animal ($n = 3$), respectively, and their viability was $95.5 \pm 0.6\%$ and $69.6 \pm 2.2\%$ ($n = 3$), respectively. Similarly, r-hepatocytes were isolated from rats 36 h after PHx. These cells were placed on nonadhesive dishes to determine their diameters as a measure of cell size. The n-, f-, and r-hepatocytes had diameters of 22.1 ± 0.2, 20.1 ± 0.2, and 21.5 ± 1.0 μm, respectively. Previously, we had found diameters of 23.2 ± 0.5 and 17.4 ± 0.0 μm for LHs and SHs, respectively (2).

The shape of contour lines in FACS analysis were variable from experiment to experiment, depending on the axis adjustment of the cell souter that is usually made and fixed in each series of experiment. We always compared the level of FL1 (autoflorescence) and SSC (granularity) of experimental cells (f- and r-hepatocytes in this study) with control cells (n-hepatocytes). It was confirmed that the similar differences of f-hepatocytes over n-hepatocytes and that of r-hepatocytes over n-hepatocytes were reproducibly observed in three independent analyses. The FACS analysis showed that f-hepatocytes were totally different from n-hepatocytes (Fig. 1A). Most of the f-hepatocytes were less granular and less autofluorescent. The FACS profile of r-hepatocytes was similar to that of n-hepatocytes, although the former contained more populations with low granularity and low autofluorescence than the latter (Fig. 1B).

Growth Ability of n- and f-Hepatocytes

The n- and f-hepatocytes were isolated from three normal rats and four CCl_4-treated rats, respectively, and then cultured with Swiss 3T3 cells in HCGM for 10 days. The ratios of the cell number at day 10 to that at day 1 were 3.5 ± 1.0 and 3.3 ± 0.1 for f- and n-hepatocytes ($n = 3$), respectively, clearly indicating similar growth ability between the two types of hepatocytes in vitro.

The growth ability in vivo was compared between n- and f-hepatocytes. DPPIV$^+$ n- and f-hepatocytes were transplanted into DPPIV$^-$ retrorsine/PHx rats via the portal vein. The livers were harvested 48 h after transplantation. The DPPIV$^+$ n- and f-hepatocytes were counted on the host liver sections. The engraftment index of f-hepatocytes obtained by two transplantation experiments was 12.3% and 7.4% (average 9.9%), which was similar to that of n-hepatocytes, 13.0% and 5.6% (9.3%). A previous study revealed that oval cells were not seen

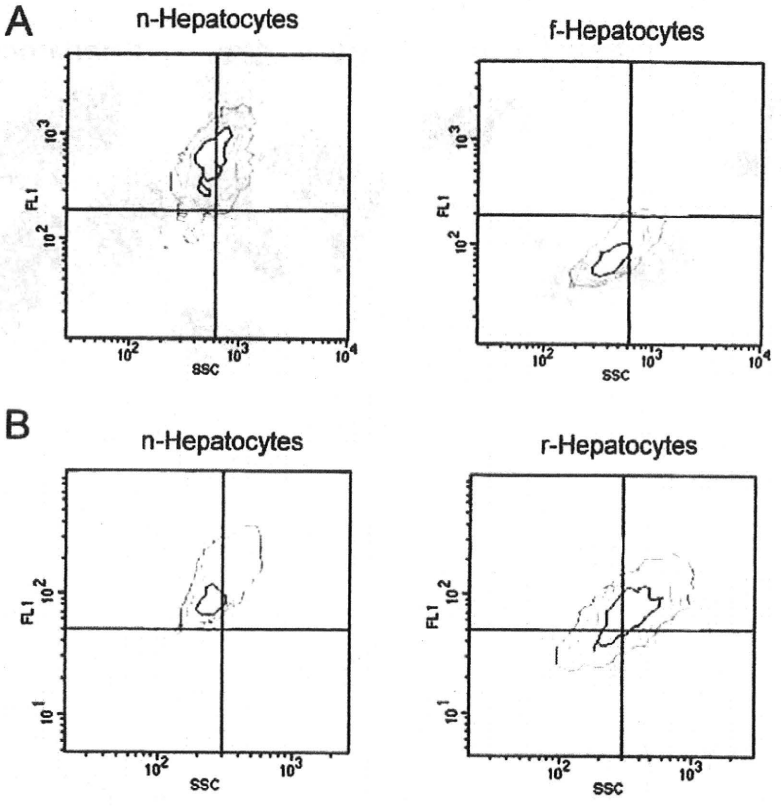

Figure 1. FACS profiles of hepatocytes. Two series (A, B) of experiments were performed in which hepatocytes were analyzed by FACS in terms of the side scatter (SSC) and fluorescence through 530-nm filter (FL1). (A) One series compared the FACS profiles of n- and f-hepatocytes, and (B) the other compared the profiles of n- and r-hepatocytes.

in the livers of CCl_4-treated rats (3). In the present study, serial liver sections were immunostained for DPPIV and an oval cell marker, OV6. There were no DPPIV and OV6 double-positive cells (data not shown), showing the absence of oval cells in the hepatocyte preparations used in this study.

Retrorsine/PHx DPPIV$^-$ rats were transplanted with n- and f-hepatocytes that had been isolated from four DPPIV$^+$ rats each as described above, killed 21 days after transplantation, and their livers were processed for DPPIV$^+$ enzyme histochemistry (Fig. 2). The f-hepatocyte colonies were more heterogeneous in size and appeared larger than the n-hepatocyte colonies, suggesting higher growth potential of the former than the latter. To quantitatively evaluate the growth ability, we measured two parameters on histological sections, the colony area and volume. Area size distribution of the hepatocyte colonies was determined and is shown in Figure 3, which confirmed the above suggestions of higher size heterogeneity and larger colony area of f-hepatocytes than those of n-hepatocytes. The mean colony area was calculated from these graphs and is shown in Table 1. f-Hepatocytes formed colonies whose areas were approximately 2.4-fold larger (significant at $p < 0.05$) than those of n-hepatocytes. The diameter of the hypothetical sphere formed by the transplanted hepatocytes was measured and also is shown in Table 1. As expected, the colony volume of f-hepatocytes was approximately 3.7-fold larger (significant at $p < 0.05$) than that of n-hepatocytes. From the mean area and volume of colonies formed by the transplanted hepatocytes, we estimated the replication potential of a transplanted cell. To simplify the calculation, we assumed that transplanted hepatocytes were spherical, and we calculated the number of transplanted cells per area and volume of a colony as described in the Materials and Methods. As shown in Table 2, the number of transplanted cells per area and volume of a colony was about 1.9- and 2.6-fold larger than that of n-hepatocytes, respectively. The average numbers of cell divisions for transplanted f- and n-hepatocytes over 21 days were calculated to be 11–13 and 9–11, respectively (Table 2). From these measurements, we concluded that f-hepatocytes have higher growth potential than n-hepatocytes in vivo.

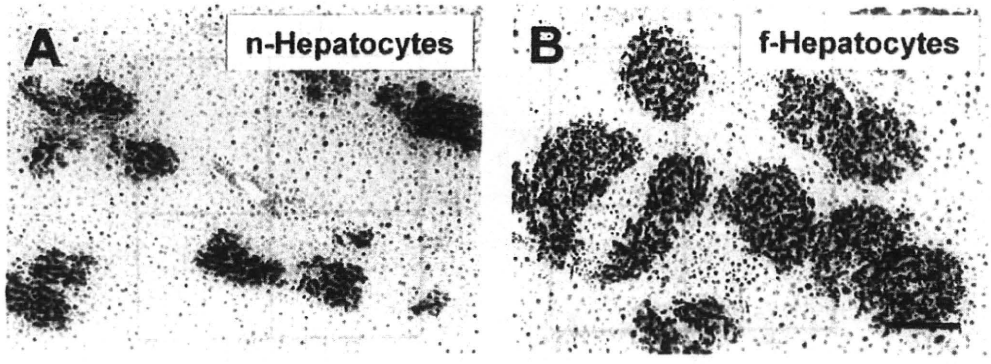

Figure 2. Colonies formed by transplanted hepatocytes. (A) DPPIV$^+$ n-hepatocytes and (B) DPPIV$^+$ f-hepatocytes were transplanted into the livers of retrorsine/PH DPPIV$^-$ rats. Liver sections were prepared from the rats 21 days after transplantation. Cryosections of the livers were subjected to DPPIV histochemical staining. The transplanted hepatocytes were stained black. Scale bar: 200 μm.

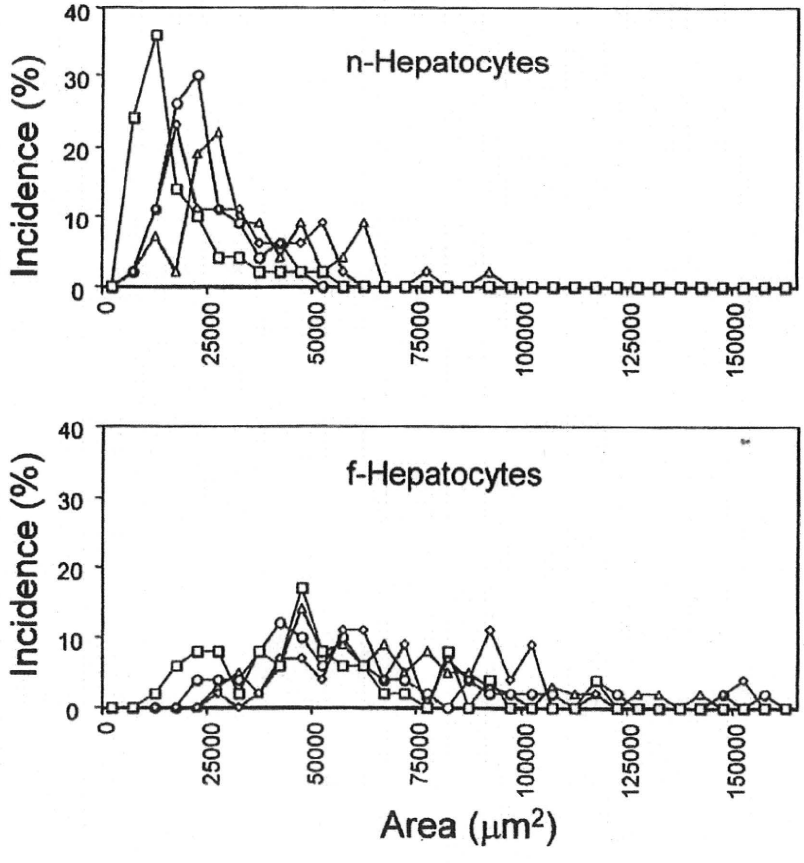

Figure 3. Size distribution of the hepatocyte colonies. Forty regions were selected randomly from DPPIV-stained sections for four individuals as shown in Figure 2 and were photographed. The colony area was measured on the photographs using NIH ver. 1.62. Each line represents the proportion (%) of the area measured for each of the four animals. f-Hepatocytes occupied more area than n-hepatocytes.

Table 1. The Mean Area and Volume of Colonies Formed by Transplanted Hepatocytes

Transplanted Cells	Area (μm^2)	Volume (μm^3)	Number
n-Hepatocytes	26,387 ± 1,015 *	3,580,888 ± 212,285 *	211
f-Hepatocytes	64,450 ± 2,016 *	13,207,708 ± 628,909 *	206

Hepatocytes were transplanted into the livers of rats, which were killed 21 days after transplantation. The areas of colonies were measured for four different rats transplanted with hepatocytes under the identical experimental conditions, as shown in Figure 2. The mean ± SE of areas and volumes of colonies was calculated from these measurements.
*$p < 0.05$. The p-values were determined by Mann-Whitney rank sum test.

Cell Phenotype in Colonies Formed by Transplanted Hepatocytes

The cells in the colonies of n- and f-hepatocytes were characterized in terms of the expression of four lineage-specific markers of liver cells: albumin, α-SMA, CK19, and GST-P. The cells in colonies of both types of hepatocytes expressed albumin at a high level, comparable to that of the surrounding host hepatocytes (Fig. 4A–D). Neither CK19 nor GST-P was expressed in the cells of colonies formed by both types of hepatocytes (data not shown), supporting the notion that f-hepatocytes do not show preneoplastic or bile duct epithelial cell phenotypes. These results strongly suggest that f-hepatocytes retain the phenotype of normal hepatocytes and maintain the normal phenotype throughout replication. In addition, α-SMA$^+$ cells (activated stellate cells) were not observed in the f-hepatocyte-transplanted livers (Fig. 4G, H) as in the n-hepatocyte-transplanted livers (Fig. 4E, F).

Gene Expression in f-Hepatocytes

Previously, we had identified 10 SH-associated genes: *p55cdc, Sta, CYP17, Pge2r, Psti, Cdc2, Cx26, Mcak, rat EST 207254*, and an unknown gene (*ab088476*) (2). The mRNA expression levels of all of these genes except *rat EST 207254* were determined using real-time RT-PCR in n-, f-, and r-hepatocytes (Fig. 5B, Table 3) and were compared with our previous data, which are shown in Figure 5A. The expression levels of the SH-associated genes were much higher in SHs than in LHs (Fig. 5A). The expression levels of four genes (*ab088476, Pge2r, Cx26*, and *Psti*) were similar between n- and f-hepatocytes. By contrast, five genes (*CYP17, p55cdc, Cdc2, Mcak*, and *Sta*) were expressed at much higher levels in f-hepatocytes than in n-hepatocytes. It was noteworthy that the overall expression profile of n-hepatocytes was similar to that of r-hepatocytes (Fig. 5B).

DISCUSSION

Fibrotic livers have been characterized mainly with respect to activated stellate cells, which are known as extracellular matrix (ECM)-producing cells, and little is known about the nature of hepatocytes in the fibrotic liver. Mito et al. reported that hepatocytes from fibrotic liver exhibited greater proliferation than hepatocytes from normal liver when transplanted into the spleen, despite the injection of approximately 1/200 of the amount of normal cells (10). Histological observations revealed that transplanted hepatocytes from cirrhotic livers differentiated into plates two to several cells thick, whereas plates of one-cell thickness prevailed with the transplantation of normal hepatocytes. One interpretation of this observation is that cirrhotic hepatocytes are still in the regenerating phase. Hepatocytes from cirrhotic livers retained normal functions such as glycogenesis and albumin synthesis (10). On electron micrographs, collagen fibers in the space of Disse were observed 1 year after the transplantation of hepatocytes from cirrhotic livers, but were not present with normal hepatocyte transplantation (10). In the present study, we characterized hepatocytes isolated from the fibrotic liver for the first time in

Table 2. Mean Cell Number in a Colony

Transplanted Cells	Cell Diameter (μm)	Cell Number per Colony Area	Cell Number per Colony Volume	Cell Divisions During 21 Days
n-Hepatocytes	22.8 ± 0.5	110 ± 12	1,217 ± 206	9–11
f-Hepatocytes	20.3 ± 0.3	209 ± 21	3,131 ± 481	11–13

Data are expressed as the mean ± SE.

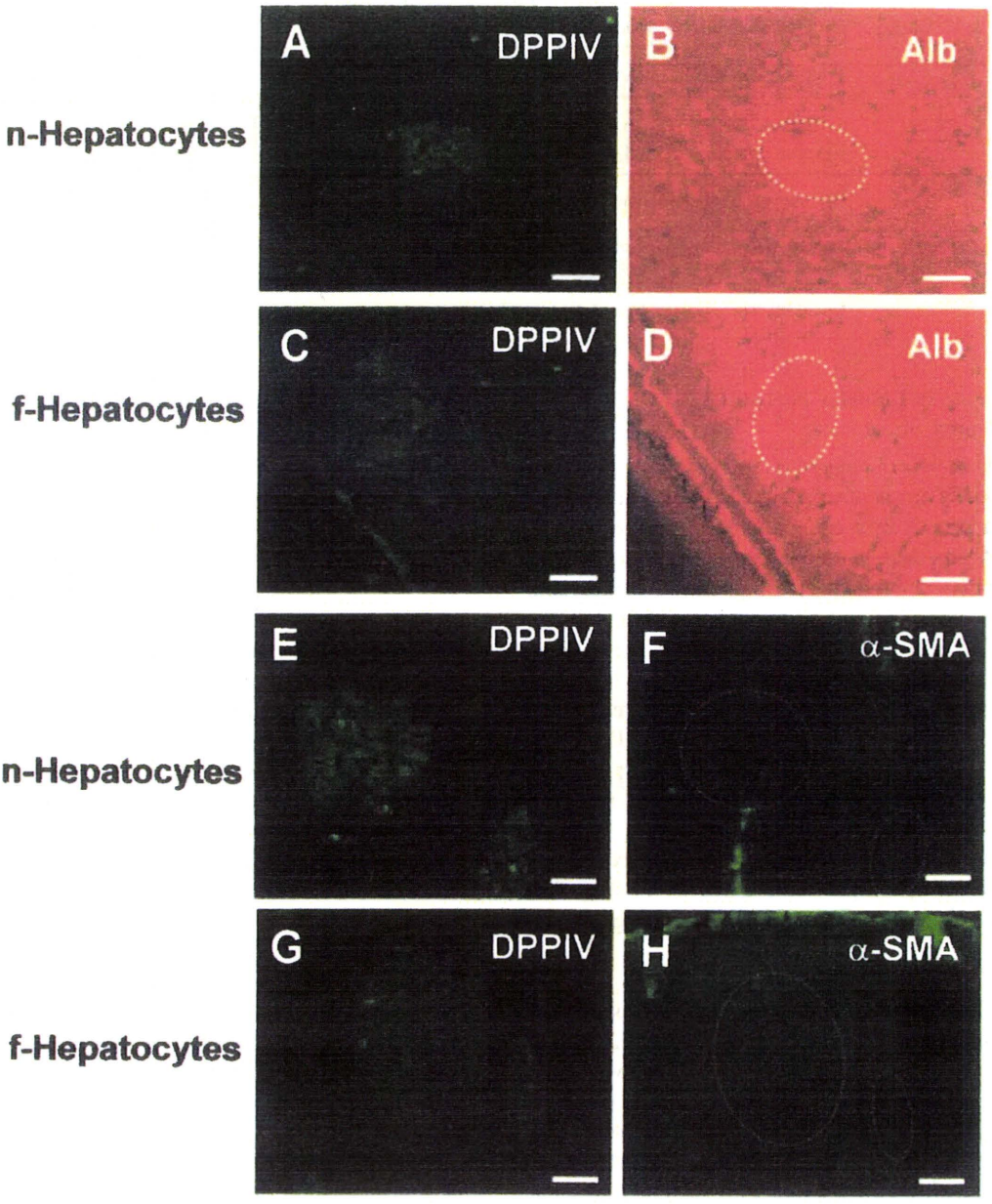

Figure 4. Phenotypes of the cells in the colonies formed by transplanted hepatocytes. DPPIV$^+$ n-hepatocytes (A, B, E, and F) and DPPIV$^+$ f-hepatocytes (C, D, G, and H) were transplanted into retrorsine/PH-treated DPPIV$^-$ rats. Serial liver cryosections were prepared 21 days after transplantation and were stained for DPPIV (A, C, E, and G), albumin (B and D), and α-SMA (F and H). The colonies formed by the transplanted hepatocytes are localized as DPPIV$^+$ regions (A, C, E, and G). These colonies are each marked by broken lines on the corresponding immunostained serial sections (B, D, F, and H). The DPPIV$^+$ cells were all albumin$^+$. There were no α-SMA$^+$ cells in the livers transplanted with both n- and f-hepatocytes. Scale bar: 100 μm.

terms of their growth potential in vitro and in vivo (in the retrorsine/PH rat liver), FACS profile, cell size, growth potential, and gene expression.

The growth potential of hepatocytes is heterogeneous: the hepatocyte with the greatest proliferative ability forms a colony consisting of more than 100 cells within 10 days, whereas the hepatocyte with the lowest ability does not divide (19). The adult rat liver contains a minor population of hepatocytes called SHs, which have a smaller size and higher replicative potential than LHs (6,17,19). Previously, we had used FACS and centrifugal elutriation to isolate highly proliferative SHs as

cells with low autofluorescence and low granularity (2). In the present study, most of the f-hepatocytes had low autofluorescence and low granularity, similar to SHs. Therefore, we investigated whether f-hepatocytes have characteristics similar to SHs in terms of size, growth potential in vitro and in vivo, and gene expression.

The average diameter of f-hepatocytes (20.1 ± 0.2 μm) was comparable to that of n-hepatocytes (22.1 ± 0.2

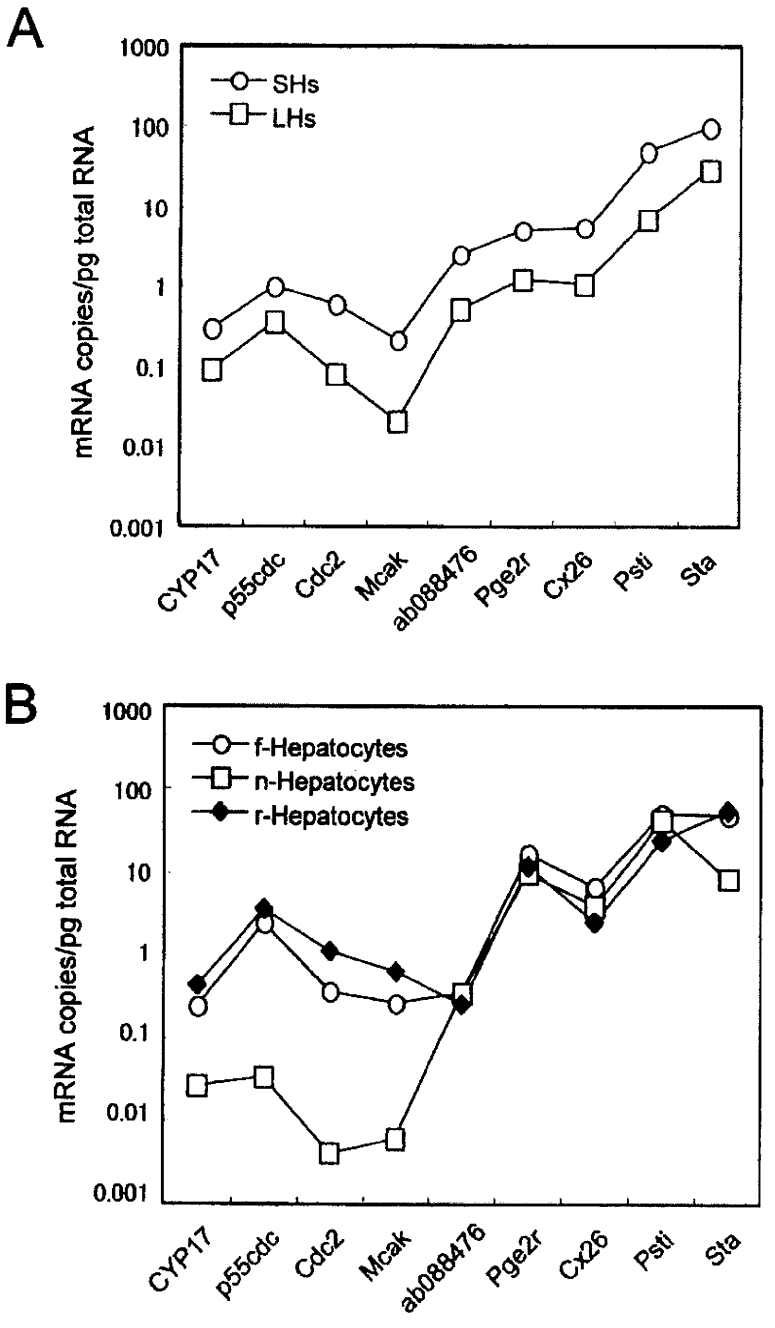

Figure 5. Expression of the SH-associated genes in hepatocytes. (A) Gene expression levels in SHs and LHs. This graph is drawn using the mRNA expression data presented in Tables 4 and 5 of Asahina et al. (2). (B) The gene expression levels in n-, f-, and r-hepatocytes were determined by measuring the mRNA copy number using real-time RT-PCR.

Table 3. Expression Levels of SH-Associated Genes in n-, r-, and f-Hepatocytes

Gene*	mRNA Copies/pg Total RNA		
	n-Hepatocytes	f-Hepatocytes	r-Hepatocytes
CYP17	0.026 ± 0.000	0.239 ± 0.147	0.430 ± 0.216
p55cdc	0.032 ± 0.022	2.443 ± 3.138	3.527 ± 1.044
Cdc2	0.004 ± 0.004	0.360 ± 0.424	1.092 ± 0.397
Mcak	0.006 ± 0.008	0.259 ± 0.308	0.627 ± 0.197
Unknown (*ab088476*)	0.343 ± 0.566	0.339 ± 0.281	0.252 ± 0.032
Pge2r	9.770 ± 8.698	16.452 ± 11.455	11.557 ± 1.699
Cx26	3.870 ± 0.967	6.690 ± 2.426	2.481 ± 0.267
Psti	40.961 ± 9.499	48.189 ± 11.954	23.374 ± 9.560
Sta	8.429 ± 7.905	46.431 ± 36.094	52.897 ± 21.741

The primers used for real-time RT-PCR have been reported elsewhere (2). Each value represents the mean ± SD of three different rats.
*Genes identified as differentially expressed using a cDNA microarray and representational difference analysis in SHs (2).

μm) but was larger than that of SHs (17.4 ± 0.0 μm). The growth of f-hepatocytes in vitro was compared with that of n-hepatocytes. Previously, we had shown that SH proliferation was about four times that of LHs in vitro (17). The f-hepatocytes showed growth ability similar to that of n-hepatocytes. SHs were also highly proliferative in vivo (about three times compared with LHs), as determined by colony-forming ability after transplantation into the livers of the retrorsine/PH rats (6). Here, we also estimated the growth potential of hepatocytes using this model. The engraftment index obtained in this study at 48 h after transplantation was 9.9% for f-hepatocytes and 9.3% for n-hepatocytes, and did not differ significantly. The colonies formed by transplanted cells at 21 days were examined in all of the residual livers of the recipients and showed that f-hepatocytes were more proliferative (about 2.5 times) than n-hepatocytes.

From the data, we concluded that f-hepatocytes have higher growth ability than n-hepatocytes in vivo but not in vitro. At present, there is no explanation for this apparent discrepancy between the in vivo and in vitro growth abilities of the two types of hepatocytes. However, it seems that the culture conditions used in the present study were not sufficient for f-hepatocytes to exhibit their full proliferation potential.

Ten SH-associated genes had been identified previously (2). We examined whether f-hepatocytes also express the SH-associated genes, and we compared the expression of SH-associated genes between f- and r-hepatocytes. The f-hepatocytes expressed five of the nine SH genes, at similar levels as SHs. Importantly, the overall expression profile of f-hepatocytes resembled that of r-hepatocytes.

The expression of marker proteins specific to hepatocytes, preneoplastic hepatocytes, and bile duct epithelial cells was characterized in f-hepatocytes. When rats were treated with CCl_4 for more than 7 weeks, morphologically recognizable GST-P$^+$ preneoplastic nodules were observed in some of the treated rats (7). In the present study, the cells in colonies formed by transplanted f-hepatocytes were albumin$^+$ but CK19$^-$ and GST-P$^-$, like n-hepatocytes, showing that the cells in the f-hepatocyte colonies expressed hepatocyte markers but not bile duct or preneoplastic markers. In addition, stellate cells did not express α-SMA in the f-hepatocyte colonies. There seems to be a regulatory mechanism in vivo under which f-hepatocytes stably express hepatocytic phenotypes but do not express biliary phenotypes.

In this study, we demonstrated that hepatocytes surrounded by ECM in the fibrotic liver retained high growth potential. f-Hepatocytes can be used instead of n-hepatocytes for hepatocyte transplantation, although the yield of hepatocytes from a fibrotic liver is fewer than that from a normal liver. However, it remains to be determined whether human f-hepatocytes have similar normal and proliferative phenotypes as rat f-hepatocytes, when isolated from the livers of fibrotic patients and transplanted into normal recipients. If they show these phenotypes, fibrotic livers could be a useful source of hepatocytes for the treatment of liver damage using hepatocyte transplantation.

ACKNOWLEDGMENTS: We thank Mss. Y. Yoshizane, H. Kohno, Y. Matsumoto, and S. Nagai for technical assistance, and Drs. M. Mito and K. Asahina for valuable advice. This work was supported by a grant from the Cooperative Link of Unique Science and Technology for Economy Revitalization (CLUSTER), Japan.

REFERENCES

1. Asahina, K.; Sato, H.; Yamasaki, C.; Kataoka, M.; Shiokawa, M.; Kataoka, S.; Tateno, C.; Yoshizato, K. Pleio-

trophin/heparin-binding growth-associated molecule as a mitogen of rat hepatocytes and its role in regeneration and development of liver. Am. J. Pathol. 160:2191–2205; 2002.
2. Asahina, K.; Shiokawa, M.; Ueki, T.; Yamasaki, C.; Aratani, A.; Tateno, C.; Yoshizato, K. Multiplicative mononuclear small hepatocytes in adult rat liver: Their isolation as a homogeneous population and localization to periportal zone. Biochem. Biophys. Res. Commun. 342: 1160–1167; 2006.
3. Dabeva, M. D.; Alpini, G.; Hurston, E.; Shafritz, D. A. Models for hepatic progenitor cell activation. Proc. Soc. Exp. Biol. Med. 204:242–252; 1993.
4. Fox, I. J.; Chowdhury, J. R.; Kaufman, S. S.; Goertzen, T. C.; Chowdhury, N. R.; Warkentin, P. I.; Dorko, K.; Sauter, B. V.; Strom, S. C. Treatment of the Crigler-Najjar syndrome type I with hepatocyte transplantation. N. Engl. J. Med. 338:1422–1426; 1998.
5. Hixson, D. C.; Chapman, L.; McBride, A.; Faris, R.; Yang, L. Antigenic phenotypes common to rat oval cells, primary hepatocellular carcinomas and developing bile ducts. Carcinogenesis 18:1169–1175; 1997.
6. Katayama, S.; Tateno, C.; Asahara, T.; Yoshizato, K. Size-dependent in vivo growth potential of adult rat hepatocytes. Am. J. Pathol. 158:97–105; 2001.
7. Kohashi, T.; Tateaki, Y.; Tateno, C.; Asahara, T.; Obara, M.; Yoshizato, K. Expression of pleiotrophin in hepatic nonparenchymal cells and preneoplastic nodules in carbon tetrachloride-induced fibrotic rat liver. Growth Factors 20: 53–60; 2002.
8. Laconi, E.; Oren, R.; Mukhopadhyay, D. K.; Hurston, E.; Laconi, S.; Pani, P.; Dabeva, M. D.; Shafritz, D. A. Long-term, near-total liver replacement by transplantation of isolated hepatocytes in rats treated with retrorsine. Am. J. Pathol. 153:319–329; 1998.
9 Lee, K. W.; Lee, J. H.; Shin, S. W.; Kim, S. J.; Joh, J. W.; Lee, D. H.; Kim, J. W.; Park, H. Y.; Lee, S. Y.; Lee, H. H.; Park, J. W.; Kim, S. Y.; Yoon, H. H.; Jung, D. H.; Choe, Y. H.; Lee, S. K. Hepatocyte transplantation for glycogen storage disease type Ib. Cell Transplant. 16: 629–637; 2007.
10. Mito, M.; Ebata, H.; Kusano, M.; Onishi, T.; Hiratsuka, M.; Saito, T. Studies on ectopic liver utilizing hepatocytes transplanted into the rat spleen. Transplant. Proc. 11:585–591; 1979.
11. Mito, M.; Kusano, M. Hepatocyte transplantation in man. Cell Transplant. 2:65–74; 1993.
12. Pertoft, H.; Smedsrød, B. Separation and characterization of liver cells. In: Pretlow, T. G.; Pretlow, T. P., eds. Cell separation, methods and selected applications, vol. 4. New York: Academic Press; 1982:1–24.
13. Sato, H.; Funahashi, M.; Kristensen, B. D.; Tateno, C.; Yoshizato, K. Pleiotrophin as a Swiss 3T3 cell-derived potent mitogen for adult rat hepatocytes. Exp. Cell Res. 246:152–164; 1999.
14. Strom, S. C.; Chowdhury, J. R.; Fox, I. J. Hepatocyte transplantation for the treatment of human disease. Semin. Liver Dis. 19:39–48; 1999.
15. Strom, S. C.; Fisher, R. A.; Rubinstein, W. S.; Barranger, J. A.; Towbin, R. B.; Charron, M.; Mieles, L.; Pisarov, L. A.; Dorko, K.; Thompson, M. T.; Reyes, J. Transplantation of human hepatocytes. Transplant. Proc. 29:2103–2106; 1997.
16. Tanaka, K.; Soto-Gutierrez, A.; Navarro-Alvarez, N.; Rivas-Carrillo, J. D.; Jun, H-S.; Kobayashi, N. Functional hepatocyte culture and its application to cell therapies. Cell Transplant. 15:855–864; 2006.
17. Tateno, C.; Takai-Kajihara, C.; Yamasaki, C.; Sato, H.; Yoshizato, K. Heterogeneity of growth potential of adult rat hepatocytes in vitro. Hepatology 31:65–74; 2000.
18. Tateno, C.; Yoshizato, K. Long-term cultivation of adult rat hepatocytes that undergo multiple cell divisions and express normal parenchymal phenotypes. Am. J. Pathol. 148:383–392; 1996.
19. Tateno, C.; Yoshizato, K. Growth and differentiation in culture of clonogenic hepatocytes that express both phenotypes of hepatocytes and biliary epithelial cells. Am. J. Pathol. 149:1593–1605; 1996.

Expert Opinion

In vivo modeling of human liver for pharmacological study using humanized mouse

Katsutoshi Yoshizato[1] & Chise Tateno

[1]*Phoenixbio Co. Ltd., Academic Advisor Office, 3-4-1, Kagamiyama, Higashihiroshima, Hiroshima 739-0016, Japan*

The liver occupies a central place in the treatment of the substances taken into the body. If we could devise an *in vivo* or *in vitro* model that perfectly mimics the naturally-created human (h) liver, the work required for making effective and safe medicines would become easier and could be undertaken more cost effectively than it is currently. Considering the advantages of *in vivo* modeling over *in vitro* modeling under the current technological state of life sciences research, we have created an experimentally workable *in vivo* h-liver model, a liver-humanized mouse, in which host hepatocytes are largely replaced with healthy normal h-hepatocytes. Xenogenic h-hepatocytes are capable of constructing a histologically normal liver by collaborating with mouse-nonparenchymal cells in an elaborately organized manner. Considering its potential use for drug development, we have extensively characterized the mouse regarding the infectivity toward h-hepatitis viruses, activities of h-enzymes in Phase I and II of drug metabolisms, and h-hepatocyte-related drug transporters. These studies indicate that the humanized mouse liver mimics h-phenotypes at a level appropriate for pharmacological studies, and, thus, can be used not only for developing new medicines, but also for examining biological and pathological mechanisms in the h-liver.

Keywords: human hepatocytes, humanized mouse, immunodeficient mouse, *in vivo* drug metabolism

Expert Opin Drug Metab. Toxicol. (2009) 5(11):1435-1446

1. Introduction

The body takes in and treats natural and artificial substances from the surrounding environment; some of the processed materials are used for life activities, while others are excreted from the body. The liver plays a central role in the processing of internalized substances (metabolism). The nominal functions of the liver are performed by a group of cells called parenchymal cells, or hepatocytes. It is well known that there are interspecies differences in the hepatic metabolic patterns of a given xenobiotic. Thus, the analytical results obtained from experiments using hepatocytes from rodents, such as rats and mice, are not always relevant in predicting the responses of human (h)-hepatocytes, indicating that h-hepatocytes are required to examine the metabolism and toxicity of a given chemical when the purpose of the study is to understand the reactions of the h-liver. However, there are also difficulties in using h-hepatocytes as an analytical tool.

In creating an *in vivo* replica of the liver, a normal, healthy human would be the ideal model; however, humans cannot serve as experimental targets. Perhaps the simple and easiest way to use h-hepatocytes for such purposes is to isolate them from an appropriate source, cultivate them for propagation and utilize them in the desired experiments. However, in doing this there are several problems,

informa
healthcare

10.1517/17425250903216564 © 2009 Informa UK Ltd ISSN 1742-5255

including the limited number of normal h-livers available, the reluctance of h-hepatocytes to replicate *in vitro* and the attenuation of a normal h-hepatocytic phenotype under *in vitro* culture conditions.

Importantly, such *in vitro* characterization of hepatocytes is insufficient to correctly understand hepatocyte function *in situ*, because their biological features such as growth, proliferation and expression of phenotypes are regulated in a complex and intricate manner by other types of liver cells (nonparenchymal cells), including resident vascular endothelial cells, stellate cells and Kupffer cells (macrophages), in addition to non-resident cells, such as immune-responsive cells. These cells are tightly associated, not only structurally, but also functionally, and constitute a well-organized biological entity, the liver. That is, hepatocytes fulfill their given tasks in the context of this specialized and unique community of different cell types. It is clear that even the most advanced modern biotechnological techniques cannot create a suitable *in vitro* environment to enable isolated populations of hepatocytes to function as they would *in vivo*; however, such cells can mimic some of their *in vivo* functions.

We accept that *in vitro* experimentation is superior to its *in vivo* counterpart in terms of understanding complex biological phenomena in that cause and effect relationships among the factors involved can be examined in a point-by-point manner. However, we are still far from the time when such complete *in vitro* experimentation will be possible. Currently, *in vivo* experimentation is considered to be better than *in vitro* experimentation for examining the normal phenotypes of hepatocytes, although the interpretation of results obtained in this way is not always simple because of the complex nature of the interactions between populations of various cell types.

Given these considerations, we sought to develop a small *in vivo* animal model for use in studying the biological and pharmaceutical phenotypes of h-hepatocytes. Additionally, for both *in vivo* and *in vitro* modeling, the development of technologies capable of producing large numbers of normal h-hepatocytes is required because normal h-hepatocytes are not readily available to researchers due to their obviously limited source. Generally, normal hepatocytes are not conducive for replicating *in vitro*, despite their high proliferative potential *in vivo*. If we could create such an animal model, h-hepatocytes could be readily propagated in a host liver.

To accomplish our goal to generate a small animal model with h-liver that can be utilized for investigation of drug metabolism, we utilized an immunodeficient and liver-injured mouse as a host. Such a mouse will be tolerant of receiving h-hepatocytes in its liver. The engrafted h-hepatocytes would be stimulated to actively proliferate in the liver because the host hepatocytes have been injured and they would repopulate the liver by expelling the not-replicable injured mouse (m)-hepatocytes. With this idea, we undertook intensive laboratory works investigating whether the xenogenic h-hepatocytes can actually collaborate with m-nonparenchymal cells in a proper fashion and reconstruct a normal liver both functionally and histologically. These works resulted in generating a mouse whose hepatocytes are mostly of human origin.

We next undertook works to test whether the chimeric liver is practically humanized and suitable for predicting h-type drug metabolism. These continuous endeavors in collaborations with researchers in pharmacological, pharmaceutical and medical areas have enabled us to launch a 'humanized mouse factory' that produces homogeneous mice in a large scale whose livers are largely repopulated with h-hepatocytes and made them available to researchers on demand for drug testing. In our experience, we are able to conclude that the factory mouse can contribute to the needs for high-throughput predictive models required for drug discovery. In this article, we overview the development in producing liver-humanized mice and their usefulness for research and development (R&D) activities in discovering new medicines that are suitable to humans.

Although this humanized mouse provides an ideal *in vivo* model of h-liver compared to other currently available ones, it has some problems to be solved in the future due to the lack of other types of h-cells and endocrinological h-factors that affect the metabolic activities of hepatocytes. Including these issues, we present our opinions regarding studies that have not been explored enough yet, but are important in making the liver humanized mouse a much better tool for pharmaceutical researches.

2. Ample regenerative capacity of hepatocytes *in vivo*

In adults, the liver is functionally very active, but largely quiescent in terms of proliferation. The turnover rate of h-hepatocytes is around 1 year in rodents [1,2]; however, the same organ is ready for rapid regeneration if the liver mass is reduced. Generally, the weight of an organ is closely related to body weight [3]. The ratio of liver:body weight ($R_{L/B}$) in humans is about 2.4 – 2.6% [4]. If the $R_{L/B}$ falls below this range, residual hepatocytes in the G0 phase of the cell cycle enter G1 and progress to S phase within 24 h. The hepatocytes will continue to replicate until the $R_{L/B}$ reaches 2.4 – 2.6%. This weight loss-induced regeneration is conserved through life, although the capacity decreases somewhat with age.

The exceptionally high regenerative capacity of the liver *in vivo* suggests a means for the abundant propagation of h-hepatocytes, starting with small numbers of h-hepatocytes in the liver of an appropriate model animal. In terms of the best species for this type of experimental design, mice or rats are preferable because they are commonly used in the laboratory. A key requirement for this type of experimental design is the availability of an immunodeficient mouse or rat whose liver is damaged and, thus, whose hepatocytes are in a proliferative phase.

If a rodent model satisfying these requirements is available, we could propagate h-hepatocytes by engrafting them in the animal model liver. The engrafted h-hepatocytes would then

proliferate and form colonies that would continue to expand, replacing damaged host hepatocytes, until the completion of the replacement. Regarding the immunodeficiency requirement, mice are superior to rats in that several mouse strains with defective immune systems have been characterized, whereas there is a dearth of immunodeficient rat strains. However, mice are less preferable from the viewpoint of generating large numbers of hepatocytes because there are far fewer cells in the small livers of mice.

3. Propagation of congenic and xenogeneic hepatocytes in a mouse model

An ideal mouse model for amplifying h-hepatocytes was discovered in a study of neonatal bleeding disorders. Albumin (Alb) promoter/enhancer-driven urokinase (Alb-uPA) gene-transgenic ($Tg_{Alb\text{-}uPA}$) mice carrying a tandem array of four murine urokinase genes controlled by the Alb promoter overproduced urokinase in their hepatocytes [5]. As a result, the livers became severely hypofibrinogenemic, which accelerated hepatocyte death through multiple undefined mechanisms involving extracellular matrix decomposition [6].

In this Tg mouse line, the functional liver deficit was thought to result in the chronic stimulation of liver growth [7]. Indeed, in hepatocytes with a stochastic deletion of the deleterious transgene, selective hepatocyte replication and expansion was observed with restoration of the liver. This event occurred most commonly in mice hemizygous for the transgene. In these animals, transgene expression in the hepatocytes was abolished because of a DNA rearrangement that affected the transgene tandem array, permitting the individuals to survive beyond birth with plasma uPA concentrations gradually returning to normal by 2 months of age. Transgene-deficient cells behaved like normal hepatocytes in transgene-active hepatocyte-induced regenerative environments, forming clonal colonies called hepatic nodules. These nodules expanded, replacing the surrounding transgene-active cells that could not replicate because of cellular damage, and eventually replaced the entire liver.

Based on this study, $Tg_{Alb\text{-}uPA}$ mice may be useful for examining the replicative capacity of hepatocytes from mice [8] and other mammals with acquired immunotolerance. Thus, when xenogeneic hepatocytes, including h-hepatocytes, were transplanted into this Tg-mouse model, the cells could be propagated at the expense of pre-existing resident hepatocytes [9].

Rhim *et al.* [10] introduced the Alb-uPA transgene into immunotolerant nu/nu mice by mating $Tg_{Alb\text{-}uPA}$ mice with Swiss athymic nude (*nu/nu*) mice, generating immunotolerant $Tg_{Alb\text{-}uPA}$ mice ($Tg_{Alb\text{-}uPA}$/NUDE mice). Rat (r) liver cells were transplanted into the livers of $Tg_{Alb\text{-}uPA}^{+/+}$/NUDE mice homozygous for the transgene. Host livers that had not been transplanted with r-liver cells were pale (white) in color. In contrast, those with r-liver cells consisted of white and red regions, with the white regions representing areas composed only of transgene-expressing host cells and the red regions representing areas composed only of transgene-deleted host m-cells, repopulated r-cells or both. Immunohistochemical analysis using antibodies against r-hepatocytes confirmed that the red regions consisted primarily of r-hepatocytes. The completely regenerated Tg m-livers resembled normal m-livers in terms of their color, shape and size. Southern blot DNA band analysis demonstrated that up to 56% of the DNA was of rat origin, in accordance with the parenchymal cell occupancy rate in the liver and supports the idea that the host liver was chimeric, with r-parenchyma and m-nonparenchyma, including vessels, bile ducts and associated connective tissues.

The weight ratio of liver:body ($R_{L/B}$) was around 7%, similar to that in the non-transgenic control mice (~ 6%), indicating that the r/m-chimeric livers were able to terminate growth normally. The successful generation of a healthy mouse with a chimeric liver indicates that r-parenchymal and m-nonparenchymal cells can communicate with each other to reconstitute a functional liver, despite the species difference. It is known that hepatocytes initiate and terminate proliferation under the influence of nonparenchymal cells [11]. Thus, the normal progress and termination of r/m-chimeric liver regeneration indicates that r-hepatocytes produce surface proteins that interact correctly with soluble m-factors, the m-extracellular matrix and m-surface proteins on m-nonparenchymal cells.

Together, these studies indicate that constitutive expression of the uPA transgene in resident m-hepatocytes generated a selective environment that favored the growth of not only endogenous m-hepatocytes with a normal (non-transgenic) phenotype [7], but also of transplanted congenic [8] and xenogeneic hepatocytes [9,10,12], raising the possibility that the liver of a uPA-Tg mouse could be reconstituted with h-hepatocytes [10]. This possibility was verified independently by two groups in 2001 [13,14] in studies of hepatitis virus infectivity.

4. Propagation of h-hepatocytes in a mouse model

Three types of immunodeficient mice have been used as hosts for h-hepatocytes. The first studies to produce a mouse with a h-hepatocyte/mouse (h/m)-chimeric liver were reported simultaneously, with one using recombinase-activating gene-2 (RAG-2)-knockout mice as the immunodeficient host [13] and the other [14] using severe combined immunodeficient (SCID) mice [15] that lacked mature B and T cells due to an inactivating mutation in the catalytic subunit of a DNA-dependent protein kinase ($Prkdc^{scid}$) [16]. Recently, an additional immunodeficient mouse strain, NOG, was used as a host; these mice lack not only mature T and B lymphocytes, but also NK cells [17]. Non-obese diabetic (NOD) mice are prone to the spontaneous development of autoimmune insulin-dependent diabetes mellitus [18]; related strains were developed at the Shionogi Research Laboratories as NOD/Shi mice. NOD/Shi mice were crossed with the SCID mice. Highly

immunodeficient mice, called NOG (NOD/Shi-*scid* IL-2Rγ^{null}) mice, were generated by backcrossing the resulting NOD/Shi-*scid* mice with IL-2 receptor γ-chain gene-knockout (C57BL/6J-IL-2Rγ^{null}) mice [19].

These three immunodeficient mice strains (RAG-2 knockout, SCID and NOG) were used as partner mouse lines for mating with the genetically liver-injured uPA-Tg mouse line. h-Hepatocytes were engrafted in the livers of these immunodeficient and liver-injured mice. h-Hepatocyte transplantation studies with uPA/RAG-2-knockout and uPA/SCID mice successfully generated mice harboring h-hepatocyte-repopulated livers. The extent of h-hepatocyte repopulation could be periodically monitored by measuring the h-Alb levels in the host blood and quantified as the replacement index (RI, the ratio of engrafted h-hepatocytes to the total number of hepatocytes (m- and h-hepatocytes) in the host liver) by calculating the ratio of the area occupied by a h-specific hepatocytic protein, such as h-cytokeratin (CK) 8/18, to the entire area in immunohistochemical sections of the host liver tissues.

In early studies, the attained RIs were between about 15 and 50% in the uPA/RAG-2-knockout and uPA/SCID mouse experiments, respectively. Three years after these two pioneering studies, we conducted additional studies using mice with h-hepatocyte-repopulated livers in an attempt to increase the RI as much as possible and to examine the possibility of using them to predict h-type metabolism and the excretion of xenobiotics [20].

As a result, we were able to generate chimeric mice having livers with RIs as high as 96%. Similarly, Meuleman *et al.* [21] made an h-liver in a uPA/SCID mouse with an RI around 90%. Suemizu *et al.* [17] transplanted h-hepatocytes into the livers of NOG mice and followed the engraftment and proliferation of the h-hepatocytes therein, generating chimeric mice with RIs up to 80%.

5. Human versus murine properties of h-hepatocyte-repopulated mouse livers

In our studies, ~ 10^6 normal viable h-hepatocytes per mouse were typically transplanted into the livers of uPA/SCID mice at 20 – 30 days after birth [20]. The h-hepatocytes engrafted the livers at rates as high as 96% and progressively repopulated them, as shown by increases in hAlb in the host blood. The actual growth of h-hepatocyte colonies was visualized and quantified in liver tissue sections from chimeric mice that had been immunohistologically stained with h-specific anti-CK8/18 antibodies. The engrafted h-hepatocytes started to proliferate around 7 days after transplantation and formed colonies, which gradually became larger, replacing the damaged host m-hepatocytes, and were nearly confluent at around day 80, when the RI reached 100% (**Figure 1A**). Histological analyses showed a well-organized hepatic architecture with normally located portal and central veins formed by m-cells, separated by intervening hepatic plates formed by h-hepatocytes (**Figure 1B**). The emergence of hepatic parenchymal cells in mice that are primarily h-hepatocytes raises an interesting biological question: do the h-hepatocytes in mouse livers remain h-hepatocytes or do they adopt the characteristics of m-hepatocytes to conform to the m-liver environment?

h-Hepatocytes are under the control of m-nonparenchymal cells in the m-liver. Thus, it is apparent that the h-hepatocytes can no longer be truly authentic h-hepatocytes, as they would be in an h-liver. Likewise, the m-liver occupied by h-hepatocytes is no longer an authentic m-liver, like the liver of a normal mouse. The h-hepatocyte host is immunotolerant and able to accept h-proteins physically, but may not accept them functionally. It is important to know how far removed the h-hepatocytes are from authentic h-hepatocytes, and how far removed the chimeric host liver is from an authentic m-liver, because the interest in creating an entity that adequately mimics an authentic h-liver for biological and pharmacological studies drove us to start this project in the first place. The last question is also important because if the degree of difference is too large, the host will not harmonize with the h-hepatocytes and will die.

6. Ability of h-hepatocytes to reconstruct an m-liver sufficiently to support mouse life without losing their h-hepatocyte phenotype

In our studies of h-hepatocyte-repopulated mice, we used actively growing young mice as hosts. These mice were able not only to survive, but also to grow, though relatively slowly, during the experimental period, reaching a body weight > 50% of the original and an RI > 90% [20]. Thus, h-hepatocytes can function like m-hepatocytes and support host growth.

It appears that most of the m-proteins responsible for host growth may be replaced with the corresponding h-proteins from h-hepatocytes, suggesting that h-hepatocytes are functionally accepted as m-hepatocytes in the m-liver community, enabling h-hepatocytes to communicate with m-nonparenchymal cells to such an extent that the liver can support the growth of a young mouse. Several lines of experimental evidence support this assertion. The host liver of the uPA/SCID mouse is congenitally damaged, and the mice showed lower levels of blood Alb and abnormally high levels of alanine aminotransferase, a biochemical indicator of liver damage, before h-hepatocyte transplantation.

The repopulation of h-hepatocytes in the liver increased the blood Alb concentration and decreased the alanine aminotransferase level, indicating that h-hepatocytes in place of m-hepatocytes improved m-liver function [20]. This is consistent with the results of histological analyses. In chimeric m-liver sections stained for type IV collagen, laminin, stabilin (a liver endothelial cell marker), BM8 (a Kupffer cell marker) and desmin (a hepatic stellate cell marker), highly organized liver structures made by xenogeneic hepatocytes and m-nonparenchymal cells were observed (data submitted). Interactions between hepatocytes and stellate cells are

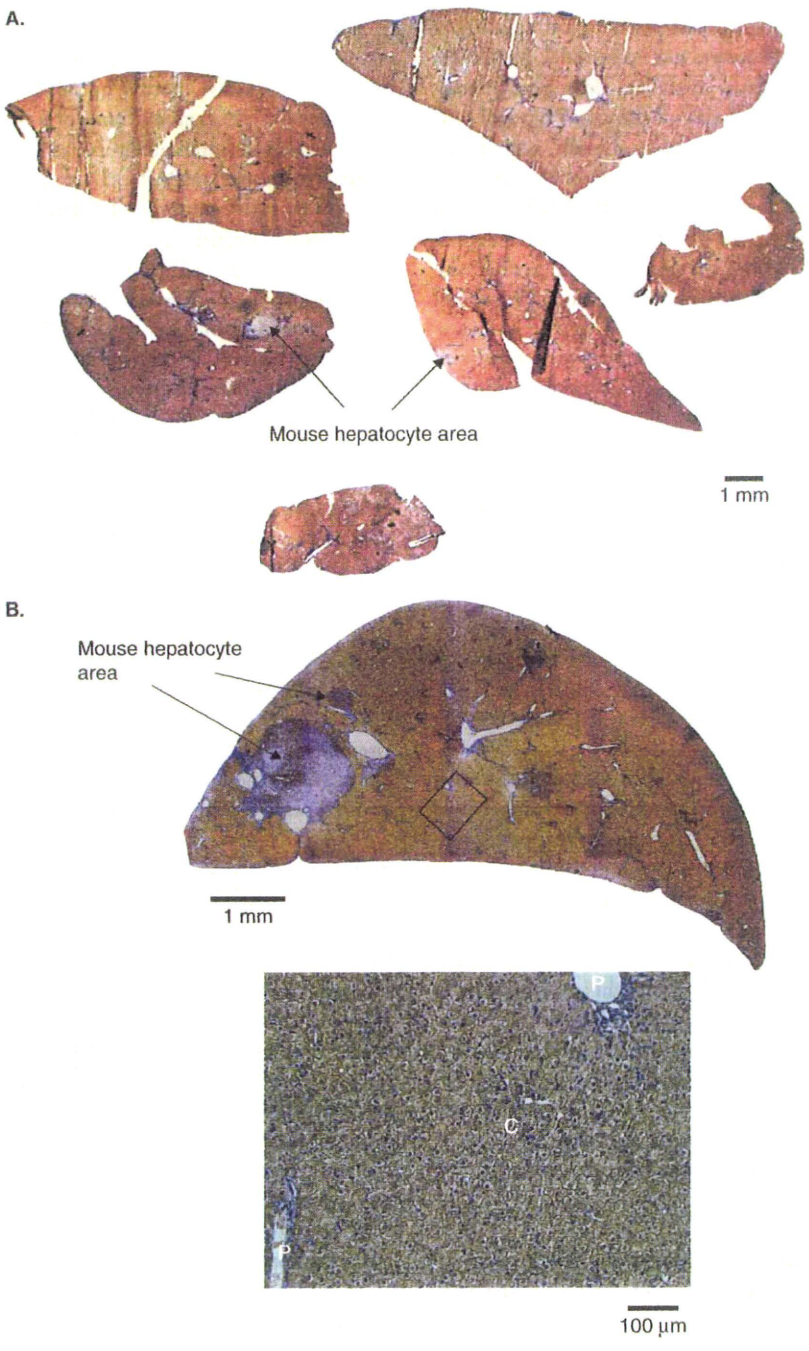

Figure 1. Appearance of m-livers constructed by xenogeneic cooperation between h-hepatocytes and m-liver nonparenchymal cells. A. h-Hepatocytes (10^6 cells) from a 6-year-old girl were transplanted into a uPA/SCID mouse. The mouse was sacrificed 77 days post-transplantation when almost all of the m-hepatocytes had been replaced with h-hepatocytes (RI = 98.8%). The six liver lobules were sectioned for h-CK8/18 staining to locate regions occupied by h-hepatocytes. Small m-hepatocytic regions remained (indicated by arrows). **B.** h-Hepatocytes (7.5×10^5 cells) from a 9-month-old boy were transplanted into a uPA/SCID mouse. The mouse was sacrificed 80 days after transplantation, when the RI reached 82%. The largest liver lobule was sectioned for h-Alb staining to locate regions occupied by h-hepatocytes. Some areas of m-hepatocytes remained (arrows, upper panel). The region enclosed by the rectangle is enlarged to show the cellular architecture (lower panel).

Bars: 1 mm for the upper panel and 100 µm for the lower panel.

C: Central vein; h: Human; m: Mouse; P: Portal vein; RI: Replacement index; SCID: Severe combined immunodeficient.